


 Cite this: *Chem. Commun.*, 2014, 50, 14674

 Received 18th September 2014,
 Accepted 7th October 2014

DOI: 10.1039/c4cc07365g

www.rsc.org/chemcomm

Two nanocage anionic metal–organic frameworks with *rht* topology and $\{[M(H_2O)_6]_6\}^{12+}$ charge aggregation for rapid and selective adsorption of cationic dyes†

 Zhifeng Zhu,^a Yue-Ling Bai,^{*a} Liangliang Zhang,^b Daofeng Sun,^{*b} Jianhui Fang^a and Shourong Zhu^{*a}

Two *rht* anionic metal–organic frameworks were synthesized. There are six $[M(H_2O)_6]^{2+}$ ions held together by a super-strong H-bond and arranged in a regular octahedron in each medium cage. Dye adsorption studies revealed a rapid and selective adsorption of cationic dyes and the adsorbed dyes can be released in saturated NaCl aqueous solution.

Metal–organic frameworks (MOFs) have received considerable attention due to their diverse structural topologies,¹ tunable porosity, and potential applications in gas adsorption/storage, separation, drug delivery and luminescence.² Considerable attention has been focused on investigating the dye adsorption from solution by MOFs in recent times.³ It is well-known that most of the dyes are very stable against light and oxidation and are difficult to degrade, making them ideal for many industrial applications. Unfortunately, many dyes are considered to be toxic and even carcinogenic.⁴ As a result of rapid development of industries including medicine, textile, leather, printing, and plastic,⁵ a large amount of industrial byproduct containing various dyes was discharged to the detriment of water quality worldwide, including China. A rapid and effective method to remove dyes from contaminated water is now a critical challenge and goal as a result. Currently, chemical, physical and biological techniques have been proposed,⁶ among these methods, adsorption rose as one of the more feasible methods thanks to its efficiency and economic competitiveness.⁷ MOFs have many advantages as adsorbents since their topological and pore characteristics are tunable by simple predesign.⁸ Further ionic MOFs may have more unique advantages such as selective adsorption of cationic or anionic dyes by host–guest electronic interactions and/or guest–guest exchange interactions.⁹

The *rht* MOFs have drawn great interest due to their unique (3,24)-connected structural features, tuneable pore size and shape, as well as adjustable host–guest interactions since the first complex was reported by Eddaoudi *et al.*¹⁰ Most research about *rht* MOFs has focused on gas adsorption¹¹ and no relevant examples about dye adsorption have been reported when this paper was written. In this paper, we use one predesigned hexacarboxylic acid ligand to synthesize two *rht* anionic MOFs with formula $[(CH_3)_2NH_2]_6[M(H_2O)_6]_3\{M_6(\eta^6-TATAT)_4(H_2O)_{12}\} \cdot xH_2O$ (1: $M = Co^{2+}$, $x = 6$; 2: $M = Ni^{2+}$, $x = 11$). These two compounds are very interesting for the following reasons: (i) they are the first example of anionic frameworks with *rht* topology; (ii) charge compensation of the anionic network relies on protonated $[(CH_3)_2NH_2]^+$ and guest $[M(H_2O)_6]^{2+}$. Unexpectedly, in each hydrophilic cage there are six $[M(H_2O)_6]^{2+}$ cations arranged in a regular octahedron formed by super-strong H-bond interactions which has not been reported previously; (iii) the skeletons maybe selectively adsorb cationic dyes in solution by guest–guest exchange. Dye adsorption studies confirmed that 1 and 2 can rapidly and selectively adsorb cationic dyes Methylene Blue (MB), Crystal Violet (CV), Malachite Green (MG), and Basic Red 2 (BR2) but hardly adsorb anionic Methyl Orange (MO), Orange II, and neutral dye molecules Methyl Red (MR) and Fluorescein (Fig. S1, ESI†) in water. It should be emphasized that most of the research about dye adsorption by MOFs are based on the size-exclusion effect and in organic solvents,^{3c–e,12} while the work about dye adsorption in water is relatively rare.^{3b,13} Selective adsorption of cationic dyes is even less common,^{3e,14} especially with CV and MG, which have high toxicity and residue characteristics that could lead to mutations and cancer. Removal of these two dyes from water is very significant.¹⁵

Compounds 1 and 2 are anionic MOFs prepared from H_6TATAT , $Co(NO_3)_2 \cdot 6H_2O$, and $Ni(NO_3)_2 \cdot 6H_2O$ in DMF– H_2O mixed solution under solvothermal conditions. The formula is determined by Single-crystal X-ray diffraction, elemental analysis and thermogravimetric analysis. The anionic framework was balanced by guest $[M(H_2O)_6]^{2+}$ and protonated $[(CH_3)_2NH_2]^+$ originating from the decomposition of DMF during the reaction. 1 and 2 are isostructural and crystallize in the cubic space group $Fm\bar{3}m$.

^a Department of Chemistry, College of Sciences, Shanghai University, Shanghai 200444, P. R. China. E-mail: yuelingbai@shu.edu.cn, shourongzhu@shu.edu.cn

^b College of Science, China University of Petroleum (East China), Qingdao, Shandong 266580, P. R. China. E-mail: dfsun@upc.edu.cn

† Electronic supplementary information (ESI) available. CCDC 1014848 and 1014849. For ESI and crystallographic data in CIF or other electronic format see DOI: 10.1039/c4cc07365g

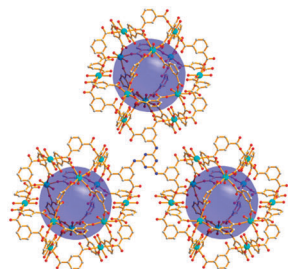


Fig. 1 3,24-connected *rht* anionic framework of **1**. Guest molecules, water molecules and H atoms have been omitted for clarity. Colour code: Co, cyan; O, red; N, blue; C gray.

In **1**, the asymmetric unit contains 1/4 Co1, 1/8 Co2, 1/6 TATAT⁶⁻ and one and a quarter of coordinated water. Co1 is coordinated to two water molecules and four carboxyl oxygen atoms from four individual TATAT⁶⁻ ligands to form a slightly distorted CoO₆ octahedral unit. The Co–O bond lengths are between 2.190(4) and 2.296(5) Å. Each TATAT⁶⁻ ligand connects six CoO₆ units resulting in an extended 3D and highly porous (3,24)-connected *rht* framework (Fig. 1), which is similar to the known *rht* topology except the electric charge.^{10,11} **1** and **2** are anionic frameworks while other *rht* networks reported are neutral or cationic frameworks balanced by the coordinated NO₃⁻.¹⁰ Co2 also possesses a slightly distorted octahedral coordination geometry, bonded by six water molecules with Co–O bond lengths ranging from 2.098(3) to 2.200(6) Å. All [Co(H₂O)₆]²⁺ ions are free and located in the medium cages (Fig. 2b).

The anionic *rht* MOF features three types of nanocages: large, truncated octahedron (T-O_h), which is composed of eight TATAT⁶⁻ ligands with a cage diameter of 2.1 nm (Fig. 2a, left); a small, truncated tetrahedron (T-T_d) is composed of four TATAT⁶⁻ ligands

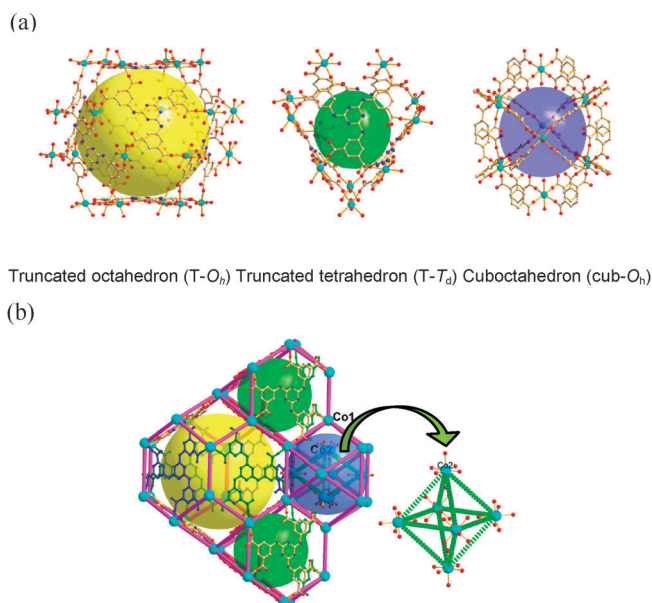


Fig. 2 (a) The large truncated octahedron (T-O_h) cage (left), small truncated tetrahedron (T-T_d) cage (middle) and medium cuboctahedron (cub-O_h) cage (right) of **1**. (b) 3D *rht* network (left) and six [Co(H₂O)₆]²⁺ arranged in a regular octahedron in medium cage (right) of **1**. Different color represents different TATAT⁶⁻ ligands.

with a 1.2 nm cage diameter (Fig. 2a, middle); and a medium, cuboctahedron (cub-O_h) is composed of 24 edges of TATAT⁶⁻ ligands with a 1.4 nm diameter (Fig. 2a, right). The T-O_h and T-T_d cages are hydrophobic while the cub-O_h cage is hydrophilic. These three cages are in a 1:2:1 ratio (Fig. 2b and Fig. S4, ESI[†]) in *rht* networks. The total accessible volume is 61.6% for **1** and 61.5% for **2** calculated by the PLATON¹⁶ after removing all of the guest molecules from the cages. It should be emphasized that all hydrated metal ions were located in the hydrophilic medium cages (cub-O_h), whose window sizes are 19.388 × 19.388 Å² (the distances between opposite atoms without consideration of Van der Waals radii). Unexpectedly, in each medium cage there are six [M(H₂O)₆]²⁺ ions which are arranged in a regular octahedron with Co2···Co2 (Ni2···Ni2) distances of 8.685 (8.672) Å. The Co2···Co1 (Ni2···Ni1) distances are 6.892 (6.883) Å (Fig. 2b). 12 positive charges within ~1.4 nm cavity have no precedence. The possible reason is that the four O4w at Co2 or Ni2 form very strong H-bonds with carboxylate O2 with an O···O distance of 2.142 or 2.139 Å as shown in Fig. S5 (ESI[†]). Generally, the O···O distance is ~2.7 Å in normal H-bonds. The strongest H-bonds may have a distance of ~2.4 Å.¹⁷ To our knowledge, this is the strongest H-bond reported until now.¹⁷ These strong H-bonds hold the six metal ions tightly in such a small cavity. The presence of these strong H-bonds is also verified by the IR spectrum with ν_{OH} at ~1101 cm⁻¹ (Fig. S6 and S7, ESI[†]),¹⁷ while there is no obvious peak at ~1101 cm⁻¹ in other TATAT-compounds.^{14,18}

Since **1** and **2** are stable and hardly soluble in common solvents including CH₂Cl₂, CHCl₃, MeOH, EtOH, DMF, acetone, and H₂O. In order to investigate the stabilities of their cages, the samples were activated by solvent-exchange with acetone, methanol, dichloromethane and chloroform. Powder X-ray diffraction (PXRD) of the activated samples shows the original sharp diffraction peaks that still exist, suggesting that the activated samples retain the crystalline structures. The PXRD results of crystals soaked in water exhibit only featureless broaden peaks and illustrate that the H₂O-soaked samples are amorphous (Fig. S8 and S9, ESI[†]). Furthermore, the thermal gravimetric analysis of as-synthesized, acetone activated, and water soaked samples **1** and **2** were investigated under a nitrogen atmosphere (Fig. S10 and S11, ESI[†]). The curves of as-synthesized **1** and **2** show a rapid weight loss and a gradual weight loss process; no obvious platforms appeared in the 25–800 °C. The acetone-activated samples **1** and **2** exhibit a first rapid weight loss process before 120 °C, corresponding to the removal of protonated dimethylamine and coordinated water. An obvious plateau appears and the framework is stable to ~380 °C, then the frameworks begin to rapidly decompose. Interestingly, the curves of water-soaked samples are similar to those of acetone-activated samples although there is no solvent exchange, which indicates that the anionic frameworks of acetone and water soaked samples can remain intact and have a good thermal stability. However, the N₂ adsorption experiments failed to give expected results to calculate the surface area, which usually happens to some highly porous MOFs, presumably because the frameworks lost their long-range order under high vacuum.^{2g,3d}

To further explore the permanent porosity, the dye adsorptions in water were investigated as dye selective adsorption is

more attractive and challenging compared to conventional dye adsorption. To evaluate whether **1** and **2** have the ability to separate dyes with similar size but different charges, eight dyes: electrically neutral MR and Fluorescein, positively charged MB, CV, MG, BR2, and negatively charged MO and Orange II, in which MB has the smallest size in cationic dyes, were chosen as the models for experiments. The as-synthesized **1** and **2** were immersed in aqueous solutions containing two dyes with different charges (MB&MR, CV&Fluorescein, MG&Orange II, BR2&MO) at room temperature respectively. Some dyes can be efficiently adsorbed within several minutes while the crystal color deepened quickly (Fig. S13, ESI[†]). The adsorption behaviors of **1** and **2** toward these dyes were recorded by UV-Vis spectroscopy (Fig. 3 and Fig. S12, ESI[†]). The results revealed that **1** and **2** can rapidly and selectively adsorb cationic dye molecules into their networks, while anionic and neutral dye molecules were left in the solution. These phenomena could be explained by the guest-guest exchange of free $[M(H_2O)_6]^{2+}$ and $[(CH_3)_2NH_2]^+$ cations in the cages with cationic dye molecules. The ICP results show that the dye molecules exchange with $[M(H_2O)_6]^{2+}$ ions preferentially when there is a small amount of adsorption, with the increase of the adsorption amount, the exchange percentage of the protonated dimethylamine is also increased (Table S2, ESI[†]). The exchange with $[M(H_2O)_6]^{2+}$ ions can be further proved by a significant decrease in strong H-bond ν_{OH} intensity at 1101 cm^{-1} (Fig. S6 and S7, ESI[†]). The adsorption rate is MB > MG > CV > BR2, resulting from the different molecular sizes of these four dyes. Generally, the adsorption capacity is greatly influenced by the concentration of the dye solutions. Here, the maximum adsorption capacity was estimated by adding 10 mg as-synthesized **1** and **2** into 10 mL of a 5 g L^{-1} dye aqueous solution for 12 h at room temperature, respectively. For **1**, the adsorption capacities for MB, CV, MG, and BR2 are 708, 607, 484 and 144 mg g^{-1} respectively. For **2**, the corresponding data are 725, 630, 502 and 152 mg g^{-1} . All these values are much higher than those observed for dye molecules on some MOFs, commercial activated carbon (Table S3, ESI[†]), and other various adsorbents. This is especially true for CV (Table S4, ESI[†])¹⁴ and MG

(Table S5, ESI[†]),¹⁹ whose maximum adsorption capacity is the highest reported. The selective adsorption is not only more efficient, but also faster. The 50% adsorption time for our system is ~ 10 min (Fig. S14 and S15, ESI[†]), while other literature reported theirs as several hours.²⁰ To date, there has been very little work about dye adsorption in aqueous solution by MOFs reported, only a few examples about their adsorption in DMF solution have been published and their reported adsorption capacities are much lower.¹⁴ Preliminary selective adsorption investigations for **1** and **2** indicate that they could be good materials in the selective removal of cationic dye molecules from polluted water, which is extremely important for contamination removal.

In order to investigate whether **1** and **2** could be recycled and reused, dye release from dye@**1** and dye@**2** was investigated and the release experiment was monitored by UV-Vis spectra. As shown in Fig. 4a and Fig. S16 (ESI[†]), the dye molecules in dye@**1** and dye@**2** could be released quickly in saturated NaCl solution. The release reached a plateau within 40 minutes except for CV, which took about 120 minutes to reach the plateau. In the deionized water the dye molecules were barely released, revealing that Na^+ could effectively facilitate the release of dye molecules. The Na^+ ions are very small compared with dye molecules and therefore it should be easy for them to enter cages to exchange the dye molecules. However, the release efficiency is not very high. For dye@**1**, the release percent is 17.9% for MB, 43.4% for CV, 40.0% for MG and 51.5% for BR2 within 120 minutes. For dye@**2**, corresponding efficiencies are 18.5%, 43.9%, 39.9% and 52.4% for MB, CV, MG and BR2 (Table S6, ESI[†]). The release ratios are ranked BR2 > CV > MG > MB. It should be mentioned that the maximum adsorption capacity and the adsorption rate of MB are larger than those of the other three dyes, and its molecular size is also the smallest. Surprisingly, the release ratio of MB is the lowest. For CV and MG, the release ratio and adsorption capacity are much higher, which indicates that **1** and **2** have much better adsorption and desorption capabilities for CV and MG. These two dyes are widely used in aquaculture as a fungicide, but because they have a high residual and toxicity characteristics as well as carcinogenic, teratogenic, and mutagenic effects, many countries have banned or restricted their use in low concentrations ($<5\text{ ppm}$). However, due to a lack of cheap and effective alternatives, they are still widely used in aquaculture. An effective removal technique from water is therefore extremely significant and necessary.

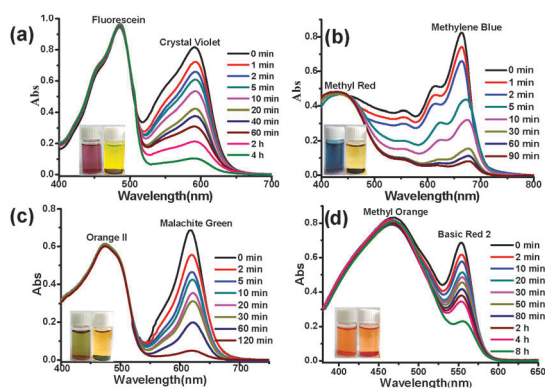


Fig. 3 UV-Vis spectral changes of 10.0 ml 8.0 ppm dye mixture in the presence of 20 mg **1**. (a) CV&Fluorescein; (b) MB&MR; (c) MG&Orange II and (d) BR2&MO. The inset photographs are before (left) and after adsorption (right).

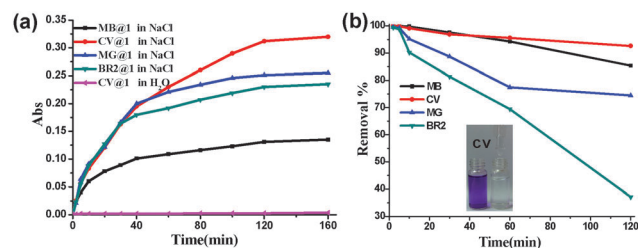


Fig. 4 (a) The dye release from dye@**1** in a saturated NaCl aqueous solution and deionized water monitored at dye's UV-Vis absorption maximum. (b) Time dependent chromatographic column efficiency determined by the absorbance before and after passing the column.

Taking into account the characteristics of rapid dye adsorption of **1** and **2**, their potential application was further investigated by column chromatography. The chromatographic columns were prepared by employing 40 mg crystals of **1** and **2** as the filler. 10 ppm dye in aqueous solution passed through the column with the flow rate of 0.5 mL min⁻¹. The UV-Vis absorbance difference of the eluent (before and after passing the column) showed the removal of MB and CV can reach 100%, and 99 and 98% for MG and BR2 within 5 minutes (Fig. 4b, Fig. S17 and S18, ESI†). With increasing time, the removal efficiency gradually decreased, especially for BR2. The percent removed is only 43% in the first 2 hours. This is still much higher in first 2 hours for CV, MB, and MG (93%, 87% and 77%), for **1** (Table S7, ESI†). The values for the column filled with **1** and **2** are basically the same (Table S8, ESI†). From the above experiments, we can further infer that **1** and **2** could serve as a good adsorbent to efficiently and selectively remove cationic dye molecules in polluted water.

In summary, two new *rht* anionic MOFs with three kinds of nanocages were synthesized and characterized. To our knowledge, they are the first examples of anionic networks with *rht* topology. Interestingly, there exist six [M(H₂O)₆]²⁺ cations arranged in a regular octahedron in each 1.4 nm hydrophilic cage. Due to the anionic network and guest cationic molecules in cages, the two compounds can rapidly and selectively adsorb cationic dyes (MB, CV, MG and BR2) by guest-guest exchange in aqueous solution. This is the first example of *rht* MOFs with high dye-adsorption efficiency and excellent selectivity in water. Of the studied dyes, CV and MG have higher adsorption and desorption capacity. These two dyes have been rarely studied. Dye adsorption and desorption studies revealed that the two compounds could be the potential functional materials to selectively remove cationic dye molecules in wastewater, which is very significant for environmental cleanup.

This work was supported by the National Natural Science Foundation of China (21001073). We thank the Instrumental Analysis and Research Center of Shanghai University for measurements.

Notes and references

- (a) J. J. Perry, J. A. Perman and M. J. Zaworotko, *Chem. Soc. Rev.*, 2009, **38**, 1400; (b) H.-C. Zhou, J. R. Long and O. M. Yaghi, *Chem. Rev.*, 2012, **112**, 673; (c) N. Stock and S. Biswas, *Chem. Rev.*, 2012, **112**, 933.
- (a) M. P. Suh, H. J. Park, T. K. Prasad and D.-W. Lim, *Chem. Rev.*, 2012, **112**, 782; (b) J.-R. Li, J. Sculley and H.-C. Zhou, *Chem. Rev.*, 2012, **112**, 869; (c) P. Horcajada, R. Gref, T. Baati, P. K. Allan, G. Maurin, P. Couvreur, G. Férey, R. E. Morris and C. Serre, *Chem. Rev.*, 2012, **112**, 1232; (d) Y. Cui, Y. Yue, G. Qian and B. Chen, *Chem. Rev.*, 2012, **112**, 1126.
- (a) R. Grunker, V. Bon, A. Heerwig, N. Klein, P. Muller, U. Stoeck, I. A. Baburin, U. Mueller, I. Senkovska and S. Kaskel, *Chem. – Eur. J.*, 2012, **18**, 13299; (b) E. Haque, J. W. Jun and S. H. Jhung, *J. Hazard. Mater.*, 2011, **185**, 507; (c) H.-N. Wang, F.-H. Liu, X.-L. Wang, K.-Z. Shao and Z.-M. Su, *J. Mater. Chem. A*, 2013, **1**, 13060; (d) M. J. Dong, M. Zhao, S. Ou, C. Zou and C. D. Wu, *Angew. Chem., Int. Ed.*, 2014, **53**, 1575; (e) R. Luo, H. Xu, H.-X. Gu, X. Wang, Y. Xu, X. Shen, W. Bao and D.-R. Zhu, *CrystEngComm*, 2014, **16**, 784.
- S. Chen, J. Zhang, C. Zhang, Q. Yue, Y. Li and C. Li, *Desalination*, 2010, **252**, 149.
- G. Crini, *Bioresour. Technol.*, 2006, **97**, 1061.
- A. Mittal, A. Malviya, D. Kaur, J. Mitta and L. Kurup, *J. Hazard. Mater.*, 2007, **148**, 229.
- M. Rafatullah, O. Sulaiman, R. Hashim and A. Ahmad, *J. Hazard. Mater.*, 2010, **177**, 70.
- J. R. Li and H. C. Zhou, *Nat. Chem.*, 2010, **2**, 893.
- (a) X.-Y. Wang, H.-Y. Wei, Z.-M. Wang, Z.-D. Chen and S. Gao, *Inorg. Chem.*, 2005, **44**, 572; (b) X.-L. Wang, C. Qin, E.-B. Wang and Z.-M. Su, *Chem. – Eur. J.*, 2006, **12**, 268.
- F. Nouar, J. F. Eubank, T. Bousquet, L. Wojtas, M. J. Zaworotko and M. Eddaoudi, *J. Am. Chem. Soc.*, 2008, **130**, 1833.
- (a) D. Yuan, D. Zhao, D. Sun and H. C. Zhou, *Angew. Chem., Int. Ed.*, 2010, **49**, 5357; (b) O. K. Farha, I. Eryazici, N. C. Jeong, B. G. Hauser, C. E. Wilmer, A. A. Sarjeant, R. Q. Snurr, S. T. Nguyen, A. O. Yazaydin and J. T. Hupp, *J. Am. Chem. Soc.*, 2012, **134**, 15016.
- (a) S. Han, Y. Wei, C. Valente, R. C. Forgan, J. J. Gassensmith, R. A. Smaldone, H. Nakanishi, A. Coskun, J. F. Stoddart and B. A. Grzybowski, *Angew. Chem., Int. Ed.*, 2011, **50**, 276; (b) Y.-Q. Lan, H.-L. Jiang, S.-L. Li and Q. Xu, *Adv. Mater.*, 2011, **23**, 5015; (c) F. Pu, X. Liu, B. L. Xu, J. S. Ren and X. G. Qu, *Chem. – Eur. J.*, 2012, **18**, 4322.
- (a) A.-X. Yan, S. Yao, Y.-G. Li, Z.-M. Zhang, Y. Lu, W.-L. Chen and E.-B. Wang, *Chem. – Eur. J.*, 2014, **20**, 6927; (b) E. Haque, V. Lo, A. I. Minett, A. T. Harris and T. L. Church, *J. Mater. Chem. A*, 2014, **2**, 193.
- C. Y. Sun, X. L. Wang, C. Qin, J. L. Jin, Z. M. Su, P. Huang and K. Z. Shao, *Chem. – Eur. J.*, 2013, **19**, 3639.
- (a) K. P. Singh, S. Gupta, A. K. Singh and S. Sinha, *J. Hazard. Mater.*, 2011, **12**, 1462; (b) B. H. Hameed and M. I. El-Khaiary, *J. Hazard. Mater.*, 2008, **154**, 237.
- PLATON: A. L. Spek, *J. Appl. Crystallogr.*, 2003, **36**, 7.
- T. Steiner, *Angew. Chem., Int. Ed.*, 2002, **41**, 48.
- (a) C.-Y. Sun, C. Qin, C.-G. Wang, Z.-M. Su, S. Wang, X.-L. Wang, G.-S. Yang, K.-Z. Shao, Y.-Q. Lan and E.-B. Wang, *Adv. Mater.*, 2011, **23**, 5629; (b) B. Y. Li, Z. J. Zhang, Y. Li, K. X. Yao, Y. H. Zhu, Z. Y. Deng, F. Yang, X. J. Zhou, G. H. Li, H. H. Wu, N. Nijem, Y. J. Chabal, Z. P. Lai, Y. Han, Z. Shi, S. H. Feng and J. Li, *Angew. Chem., Int. Ed.*, 2012, **51**, 1412.
- B. H. Hameeda and M. I. El-Khaiary, *J. Hazard. Mater.*, 2008, **02**, 54.
- J. T. Jia, F. X. Sun, T. Borjigin, H. Ren, T. T. Zhang, Z. Bian, L. X. Gao and G. S. Zhu, *Chem. Commun.*, 2012, **48**, 6010.